CISM International Centre for Mechanical Sciences 595
Courses and Lectures

Michael Le Bars
Daniel Lecoanet *Editors*

Fluid Mechanics of Planets and Stars

International Centre for Mechanical Sciences

Springer

CISM International Centre for Mechanical Sciences

Courses and Lectures

Volume 595

For more than 40 years the book series edited by CISM, “International Centre for Mechanical Sciences: Courses and Lectures”, has presented groundbreaking developments in mechanics and computational engineering methods. It covers such fields as solid and fluid mechanics, mechanics of materials, micro- and nanomechanics, biomechanics, and mechatronics. The papers are written by international authorities in the field. The books are at graduate level but may include some introductory material.

More information about this series at http://www.springer.com/series/76

Michael Le Bars · Daniel Lecoanet
Editors

Fluid Mechanics of Planets and Stars

Springer

Editors
Michael Le Bars
IRPHE (UMR 7342)
CNRS, Aix Marseille University
Centrale Marseille
Marseille, France

Daniel Lecoanet
Department of Astrophysical Sciences
Princeton University
Princeton, NJ, USA

ISSN 0254-1971 ISSN 2309-3706 (electronic)
CISM International Centre for Mechanical Sciences
ISBN 978-3-030-22073-0 ISBN 978-3-030-22074-7 (eBook)
https://doi.org/10.1007/978-3-030-22074-7

This Springer imprint is published by the registered company Springer Nature Switzerland AG
The registered company address is: Gewerbestrasse 11, 6330 Cham, Switzerland

Preface

The course "Fluid mechanics of planets and stars" was held at the International Centre for Mechanical Sciences in Udine, Italy, from April 16 to 20, 2018. It was part of the research project FLUDYCO, supported by the European Research Council (ERC) under the European Union's Horizon 2020 research and innovation program.

The scientific focus of this course was the dynamics of planetary and stellar fluid layers, including atmospheres, oceans, iron cores, convective and radiative zones in stars, etc. Our first motivation for organizing this school came from the following ascertainment: this scientific domain is by its essence interdisciplinary and multi-method. But while much effort has been devoted to solving open questions within the various communities of Mechanics, Applied Mathematics, Engineering, Physics, Planetary and Earth Sciences, Astrophysics, and while much progress has been made within each enclosed domain using theoretical, numerical, and experimental approaches, cross-fertilizations have remained marginal. The objective of this CISM School was to go beyond this state, by providing participants with a global introduction and an up-to-date overview of relevant studies, fully addressing the wide range of involved disciplines and methods.

44 participants attended the 35 lectures given by 6 lecturers, chosen so as to cover the widest possible range of skills and knowledge in fundamental mechanics as well as geo- and astrophysical applications. Professor Gordon Ogilvie from University of Cambridge (UK) was in charge of the theme "Waves in fluids and in stellar interiors". Dr. Daniel Lecoanet from Princeton University (USA) focused on the dynamics and interactions of convective and radiative zones in stars. Professor Bruce Sutherland from University of Alberta (Canada) provided an overview of instabilities in atmospheres and oceans. Dr. Michael Le Bars from CNRS (France) reviewed numerous instabilities in planetary interiors. Dr. Renaud Deguen from University Claude Bernard (France) discussed various aspects of the fluid mechanics of planetary cores. And finally, Dr. Benjamin Favier from CNRS (France) offered a large overview of various aspects of turbulences. All lectures were stimulating, of the top scientific level, and entertaining, while simultaneously highlighting the many

connections between different fields and communities. The six chapters of this book summarize this intense, but scientifically enlightening week.

Before starting, let us thank all the people from the International Centre for Mechanical Sciences, and especially its highly qualified and sympathetic secretariat, who allowed us to focus on science and made this week highly enjoyable for all participants.

Marseille, France — Michael Le Bars
Princeton, USA — Daniel Lecoanet

Contents

Chapter 1
Internal Waves and Tides in Stars and Giant Planets

Gordon I. Ogilvie

Abstract Internal waves play an important role in tidal dissipation in stars and giant planets. This chapter provides a pedagogical introduction to the study of astrophysical tides, with an emphasis on the contributions of inertial waves and internal gravity waves.

Introduction to Internal Waves

Internal waves are those restored by Coriolis or buoyancy forces in rotating or stably stratified fluids. In stars and giant planets, internal waves can propagate at frequencies that are much lower than those of acoustic or surface gravity waves and are usually more suitable for excitation by tidal forcing when the body has a close orbital companion. I begin this chapter with an exploration of some of the basic properties of internal waves, using the simplest possible models.

Plane Inertial Waves

Consider an unbounded, inviscid, incompressible fluid that is rotating uniformly with angular velocity $\boldsymbol{\Omega}$. In the rotating frame, arbitrary velocity perturbations $\boldsymbol{u}$ to this basic state satisfy the equation of motion and incompressibility condition

$$\frac{D\boldsymbol{u}}{Dt} + 2\boldsymbol{\Omega} \times \boldsymbol{u} = -\nabla q, \qquad \nabla \cdot \boldsymbol{u} = 0,$$

where $D/Dt = \partial/\partial t + \boldsymbol{u} \cdot \nabla$ is the Lagrangian time derivative and q is the pressure perturbation divided by the density. Initially neglecting the nonlinear term $\boldsymbol{u} \cdot \nabla \boldsymbol{u}$,

G. I. Ogilvie (✉)
DAMTP, Cambridge, UK
e-mail: gio10@cam.ac.uk

M. Le Bars and D. Lecoanet (eds.), *Fluid Mechanics of Planets and Stars*,
CISM International Centre for Mechanical Sciences 595,
https://doi.org/10.1007/978-3-030-22074-7_1

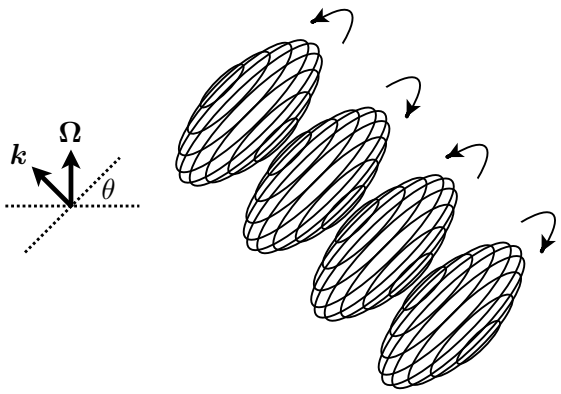

Fig. 1.1 Illustration of the fluid motion in a plane inertial wave

let us seek plane-wave solutions with wavevector $\boldsymbol{k}$ and angular frequency ω:

$$\boldsymbol{u} = \mathrm{Re}\left[\tilde{\boldsymbol{u}}\, e^{i(\boldsymbol{k}\cdot\boldsymbol{x}-\omega t)}\right], \qquad q = \mathrm{Re}\left[\tilde{q}\, e^{i(\boldsymbol{k}\cdot\boldsymbol{x}-\omega t)}\right].$$

Choosing axes such that $\boldsymbol{\Omega} = \Omega\, \boldsymbol{e}_z$, we obtain the algebraic equations

$$\begin{aligned} -i\omega\tilde{u}_x - 2\Omega\tilde{u}_y &= -ik_x\tilde{q}, \\ -i\omega\tilde{u}_y + 2\Omega\tilde{u}_x &= -ik_y\tilde{q}, \\ -i\omega\tilde{u}_z &= -ik_z\tilde{q}, \\ i\boldsymbol{k}\cdot\tilde{\boldsymbol{u}} &= 0, \end{aligned}$$

for which a non-zero solution exists if the dispersion relation

$$\omega^2 = 4\Omega^2\left(\frac{k_z^2}{k_x^2+k_y^2+k_z^2}\right)$$

is satisfied. This can be written in the form $\omega = \pm 2\Omega\cos\theta$, where θ is the angle between $\boldsymbol{k}$ and $\boldsymbol{\Omega}$.

These *plane inertial waves* (Fig. 1.1) are in fact exact solutions of the nonlinear equations (although a superposition of plane waves is not); the $\boldsymbol{u}\cdot\nabla\boldsymbol{u}$ term vanishes because $\boldsymbol{u} \perp \boldsymbol{k}$.

Plane Internal Gravity Waves

Now consider a stratified atmosphere in a uniform gravitational field $-g\,\boldsymbol{e}_z$. In the Boussinesq approximation (which is valid for highly subsonic motions on scales that are small compared to the scale height of the atmosphere), an ideal fluid satisfies the equations

$$\frac{D\boldsymbol{u}}{Dt} = -\boldsymbol{\nabla} Q + B\,\boldsymbol{e}_z, \qquad \frac{DB}{Dt} = 0, \qquad \boldsymbol{\nabla}\cdot\boldsymbol{u} = 0,$$

where Q is a modified pressure and

$$B = g\left(\frac{\rho_0 - \rho}{\rho_0}\right)$$

is a buoyancy variable, proportional to the difference between a constant reference density ρ_0 and the actual density ρ of the fluid.

An equilibrium atmosphere is a solution depending only on z, in which $\boldsymbol{u} = \boldsymbol{0}$, $Q = Q(z)$ and $B = B(z)$, with $dQ/dz = B$. Arbitrary perturbations $\boldsymbol{u}$, q and b to this basic state satisfy the nonlinear equations

$$\frac{D\boldsymbol{u}}{Dt} = -\boldsymbol{\nabla} q + b\,\boldsymbol{e}_z, \qquad \frac{Db}{Dt} + N^2 u_z = 0, \qquad \boldsymbol{\nabla}\cdot\boldsymbol{u} = 0,$$

where $N^2 = dB/dz$ is the square of the buoyancy frequency.

In the case of uniform stable stratification, N^2 is a positive constant. Initially neglecting the nonlinear terms $\boldsymbol{u}\cdot\boldsymbol{\nabla}\boldsymbol{u}$ and $\boldsymbol{u}\cdot\boldsymbol{\nabla} b$, let us seek plane-wave solutions

$$\boldsymbol{u} = \mathrm{Re}\left[\tilde{\boldsymbol{u}}\, e^{i(\boldsymbol{k}\cdot\boldsymbol{x}-\omega t)}\right],$$

etc., leading to the algebraic equations

$$-i\omega\tilde{u}_x = -ik_x\tilde{q}, \qquad -i\omega\tilde{u}_y = -ik_y\tilde{q}, \qquad -i\omega\tilde{u}_z = -ik_z\tilde{q} + \tilde{b},$$
$$-i\omega\tilde{b} + N^2\tilde{u}_z = 0, \qquad i\boldsymbol{k}\cdot\tilde{\boldsymbol{u}} = 0.$$

A non-zero solution exists if the dispersion relation

$$\omega^2 = N^2\left(\frac{k_x^2 + k_y^2}{k_x^2 + k_y^2 + k_z^2}\right)$$

is satisfied. This can be written in the form $\omega = \pm N\sin\theta$, where θ is the angle between $\boldsymbol{k}$ and $\boldsymbol{g}$.

These *plane internal gravity waves* are also exact solutions of the nonlinear equations; the $\boldsymbol{u}\cdot\boldsymbol{\nabla}\boldsymbol{u}$ and $\boldsymbol{u}\cdot\boldsymbol{\nabla} b$ terms vanish because $\boldsymbol{u}\perp\boldsymbol{k}$.

Properties of Internal Waves

There is a close similarity between the dispersion relations of inertial and internal gravity waves. These internal waves have properties that are opposite to those of acoustic or electromagnetic waves, being strongly anisotropic and dispersive. Their

frequency is independent of the magnitude $k = |\boldsymbol{k}|$ of the wavevector and depends only on its direction $\hat{\boldsymbol{k}} = \boldsymbol{k}/k$. This means that the group velocity $\partial\omega/\partial\boldsymbol{k}$ is perpendicular to $\boldsymbol{k}$ and is proportional to the wavelength $2\pi/k$. The frequency is also bounded (by 2Ω or N, respectively), resulting in a dense or continuous spectrum when suitable boundary conditions are imposed.

Linear inertial waves satisfy the differential equation

$$\frac{\partial^2}{\partial t^2}\nabla^2 q + 4\Omega^2\frac{\partial^2 q}{\partial z^2} = 0.$$

If the time-dependence $e^{-i\omega t}$ is assumed, this reduces to *Poincaré's equation*,

$$\omega^2\nabla^2 q = 4\Omega^2\frac{\partial^2 q}{\partial z^2}. \tag{1.1}$$

In frequency range $-2\Omega < \omega < 2\Omega$, this equation is hyperbolic in the *spatial* coordinates. Its characteristic curves or surfaces are inclined at a constant angle θ to the plane perpendicular to the rotation axis, where $\omega = \pm 2\Omega\cos\theta$, and coincide with the rays determined from the dispersion relation and group velocity. However, when we seek modal solutions in a contained fluid, the boundary conditions are specified on a closed surface, which is generally unsuitable for a hyperbolic equation because of the way information is propagated along the characteristics from one part on the boundary to another. The problem is generally ill-posed and smooth modal solutions may not exist; similar considerations apply to internal gravity waves.

Internal Wave Beams

An internal wave beam can be formed from a superposition of waves with the same ω and $\hat{\boldsymbol{k}}$, but different k. Consider inertial waves:

$$\frac{D\boldsymbol{u}}{Dt} + 2\boldsymbol{\Omega}\times\boldsymbol{u} = -\boldsymbol{\nabla}q, \qquad \boldsymbol{\nabla}\cdot\boldsymbol{u} = 0.$$

For waves of frequency $\omega = 2\Omega\cos\theta$, the beam is inclined at an angle θ to the horizontal. Introduce coordinates parallel (ξ) and perpendicular (η) to the beam in the xz plane, with $\boldsymbol{\Omega} = \Omega\,\boldsymbol{e}_z$ (Fig. 1.2):

$$\xi = x\cos\theta + z\sin\theta, \qquad \eta = x\sin\theta - z\cos\theta.$$

In these coordinates, we can find solutions with $u_\eta = 0$ that are independent of ξ and y, oscillating at frequency ω and satisfying

$$\frac{\partial u_\xi}{\partial t} - \omega u_y = 0, \qquad \frac{\partial u_y}{\partial t} + \omega u_\xi = 0, \qquad -\omega u_y\tan\theta = -\frac{\partial q}{\partial\eta}.$$

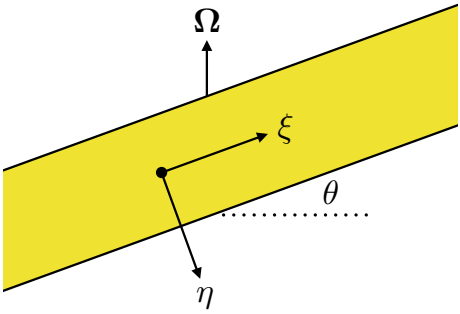

Fig. 1.2 Coordinates parallel and perpendicular to an internal wave beam

Any complex beam profile $u_\xi = \mathrm{Re}\left[U(\eta)\, e^{-i\omega t}\right]$ allows an exact nonlinear solution.

When a small viscosity ν is included, a monochromatic beam spreads as it propagates, and is accompanied by a small transverse velocity u_η. It is described approximately by

$$(u_\xi, u_\eta, u_y, q) = \mathrm{Re}\left[\left(\frac{\partial\Psi}{\partial\eta}, -\frac{\partial\Psi}{\partial\xi}, -i\frac{\partial\Psi}{\partial\eta}, -i\omega\Psi\tan\theta\right) e^{-i\omega t}\right],$$

where $\Psi(\xi, \eta)$ is a streamfunction that varies more rapidly with η than with ξ. Viscous spreading of the beam along its length is described by the equation

$$\frac{\partial\Psi}{\partial\xi} = i\lambda\frac{\partial^3\Psi}{\partial\eta^3}, \qquad \lambda = \frac{\nu}{\omega\tan\theta},$$

which can be derived by an asymptotic expansion of the solution in the limit of small viscosity. If $\lambda > 0$, then waves propagating in the $+\xi$ direction have negative transverse wavenumbers $k_\eta < 0$ and are attenuated in the $+\xi$ direction. As $\xi \to +\infty$, a generic beam tends towards a similarity solution proportional to

$$\int_{-\infty}^{0} e^{\lambda k^3\xi} e^{ik\eta}\, dk = (\lambda\xi)^{-1/3} f(\tilde{\eta}),$$

where

$$f(\tilde{\eta}) = \int_0^\infty e^{-\tilde{k}^3} e^{-i\tilde{k}\tilde{\eta}}\, d\tilde{k}, \qquad \tilde{k} = -(\lambda\xi)^{1/3}k, \qquad \tilde{\eta} = \eta(\lambda\xi)^{-1/3}$$

is a complex function (Moore and Saffman 1969) describing the transverse structure of the spreading beam in a dimensionless similarity variable (Fig. 1.3). The width of the beam is proportional to $\xi^{1/3}$, where ξ is measured along the beam from its (virtual) source. This type of structure is commonly seen in problems in which internal waves are generated by periodic forcing, as described below in the section 'Forced Internal Waves'.

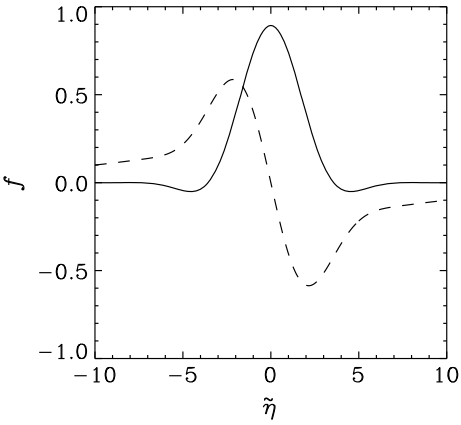

Fig. 1.3 Complex wave profile across a spreading internal wave beam. The real and imaginary parts of $f(\tilde{\eta})$ are shown as solid and dashed curves

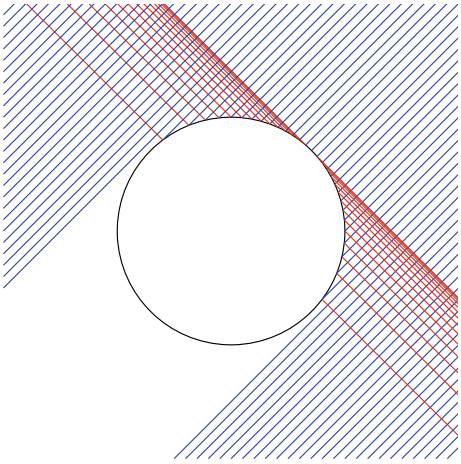

Fig. 1.4 Formation of a singularity at the critical latitude through reflection of inertial waves from a sphere. Rays incident from the top right are blue and rays reflected from the sphere are red

Reflections and Singularities

When a beam of internal waves reflects from a boundary, preservation of the frequency and therefore of the angle between $\boldsymbol{k}$ and $\boldsymbol{\Omega}$ (or $\boldsymbol{g}$) means that the reflection is generally non-specular and leads to focusing or defocusing of the beam. Reflection of inertial waves from a sphere creates a singularity at the *critical latitude* (at which the rays are tangent to the boundary) through this focusing effect (Fig. 1.4).

In a closed container in which the boundaries are not all parallel or perpendicular to $\boldsymbol{\Omega}$ (or $\boldsymbol{g}$), internal waves are generically focused into stable limit cycles known as *wave attractors* (Maas and Lam 1995). A simple example is a square container that is tilted with respect to the axis of rotation (or gravity). In the left panel of Fig. 1.5, for the purposes of illustration, the tilt angle is $\arctan(1/3)$ and the wave frequency has been chosen to be $1/\sqrt{2}$ of the maximum frequency so that the rays propagate at

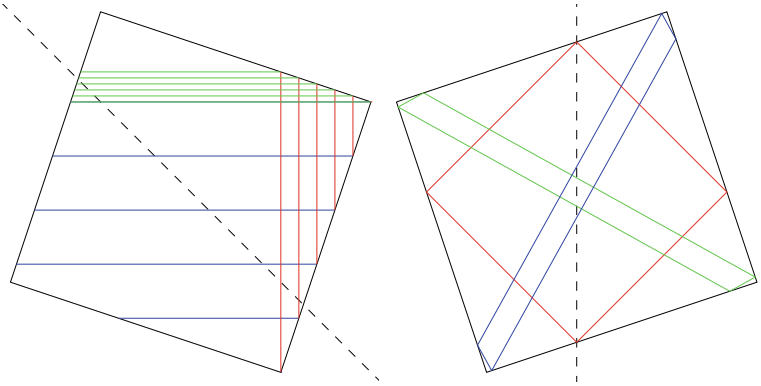

Fig. 1.5 Left: Formation of a wave attractor through focusing reflections. The dashed line indicates the axis of rotation (or gravity). The figure is oriented so that the rays propagate either horizontally or vertically. Right: Variation of the attractor with wave frequency

45° with respect to the axis. For ease of visualization, the figure is oriented so that the rays propagate either horizontally or vertically. Consider the blue rays propagating towards the right; at each reflection (producing the red rays, then the green ...), the width of the beam is halved and the rays are focused towards a square attractor. As the wave frequency is varied in the range $1/\sqrt{5} < \omega/\omega_{\max} < 2/\sqrt{5}$ (right panel, where the axis is drawn vertically), the attractor maintains a continuous existence, transforming through a family of parallelograms. The central member of the family is the square attractor, which has a total focusing power of 16 (this being the factor by which the width of the beam is reduced after a complete circuit). The outer extremes of this family are the two diagonals of the box, each of which has a total focusing power of 49.

The propagation of inertial waves in a uniformly rotating spherical shell involves both critical-latitude singularities and wave attractors (Rieutord et al. 2001). As an example of the complexity of this behaviour, Fig. 1.6 shows the frequency dependence of a measure of the focusing power of the strongest attractor, in a spherical shell with a radius ratio of $1/2$. The bandwidth of each attractor is relatively small because of the sensitivity of the trajectories of the waves to the angle of propagation and therefore to the wave frequency.

Inertial Waves in a Sphere

A problem that can be solved analytically is to find inertial wave modes in a uniformly rotating, homogeneous, incompressible fluid in a spherical container. Despite the ill-posedness of the eigenvalue problem, there does exist a complete set of modes (Ivers et al. 2015), whose frequencies are dense in the interval $-2\Omega < \omega < 2\Omega$ and

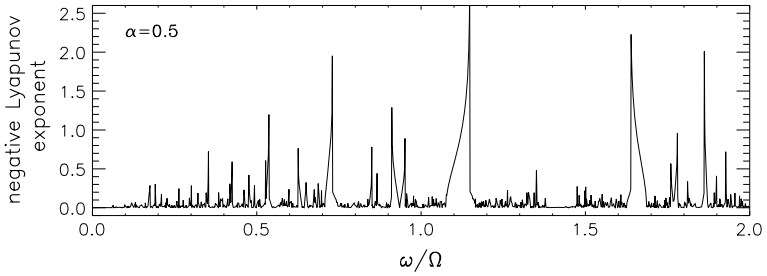

Fig. 1.6 Focusing power of the strongest inertial wave attractors in a spherical shell, as a function of wave frequency. The quantity plotted is the natural logarithm of the focusing power, divided by the number of reflections on the outer sphere; this picks out the strongest and shortest attractors. The radius ratio of the shell is 1/2

whose eigenfunctions are orthogonal polynomial vector fields. Similar results hold for an ellipsoidal container (Backus and Rieutord 2017), and appear plausible for a Maclaurin spheroid, which is a self-gravitating, homogeneous, incompressible fluid body with a free surface (Bryan 1889). Qualitatively similar modes have been found analytically in certain non-uniform spheres (Wu 2005) and computed in polytropes (Lockitch and Friedman 1999), both in a low-frequency approximation that excludes acoustic and surface gravity waves.

There are numerous methods to describe these special solutions. One is to transform Poincaré's equation (1.1), for $-2\Omega < \omega < 2\Omega$, into Laplace's equation by rescaling the z coordinate by an imaginary factor: $(\tilde{x}, \tilde{y}, \tilde{z}) = (x, y, i\alpha z)$. The homogeneous solutions of this equation that are regular at the origin are of the form $q \propto \tilde{r}^l Y_l^m(\tilde{\theta}, \tilde{\phi})$, where $\tilde{r} = \sqrt{\tilde{x}^2 + \tilde{y}^2 + \tilde{z}^2} = \sqrt{x^2 + y^2 - \alpha^2 z^2}$ is the new radial coordinate and Y_l^m is a spherical harmonic. These solutions are polynomial in $\tilde{\boldsymbol{x}}$ and therefore in $\boldsymbol{x}$. (The homogeneous solutions that are regular at infinity are of the form $q \propto \tilde{r}^{-(l+1)} Y_l^m(\tilde{\theta}, \tilde{\phi})$, but these involve negative powers of $\tilde{r}$ and therefore have singularities on the cones $\tilde{r} = 0$; as argued by Goodman and Lackner (2009), this property explains why non-singular modes cannot be found in a spherical shell.)

It is also possible to find the modal solutions by directly calculating the radial velocity in spherical polar coordinates (Ogilvie 2009). For example, in the case $m = 2$ one separable solution has

$$u_r \propto r Y_2^2$$

and another has

$$u_r \propto r^3 \left[Y_2^2 + \left(\frac{7\omega^2 + 7\Omega\omega - 2\Omega^2}{6\sqrt{3}\,\Omega^2} \right) Y_4^2 \right].$$

For free modes in a full sphere of radius R with a rigid outer boundary, u_r must vanish at $r = R$. This is possible using a linear combination of these solutions:

$$u_r \propto r(R^2 - r^2)Y_2^2,$$

when ω is one of the two roots of

$$7\omega^2 + 7\Omega\omega - 2\Omega^2 = 0, \qquad \text{i.e.} \quad \omega = \left(-1 \pm \sqrt{\frac{15}{7}}\right)\frac{\Omega}{2}.$$

These are two of the lowest order inertial modes of a full sphere.

Instabilities of Internal Waves

If internal waves exceed a critical amplitude, they break and are strongly dissipated. In the case of a stably stratified atmosphere with a plane internal gravity wave, the total buoyancy is

$$B = N^2 z + \mathrm{Re}\left[\tilde{b}\, e^{i(\boldsymbol{k}\cdot\boldsymbol{x}-\omega t)}\right] + \text{constant}.$$

The vertical gradient

$$\frac{\partial B}{\partial z} = N^2 + \mathrm{Re}\left[ik_z\tilde{b}\, e^{i(\boldsymbol{k}\cdot\boldsymbol{x}-\omega t)}\right]$$

becomes inverted at some phase if $|k_z\tilde{b}| > N^2$ (Fig. 1.7). This leads to a local convective instability that generates small-scale motions and causes the wave to break. The breaking criterion is equivalent to $|k_z\tilde{\xi}_z| > 1$, where $\boldsymbol{\xi}$ is the displacement, related to the velocity perturbation by $\boldsymbol{u} = \partial\boldsymbol{\xi}/\partial t$.

Similarly, for a plane inertial wave, the vertical component of the absolute vorticity is

$$2\Omega + \mathrm{Re}\left[i(k_x\tilde{u}_y - k_y\tilde{u}_x)\, e^{i(\boldsymbol{k}\cdot\boldsymbol{x}-\omega t)}\right]$$

and becomes inverted at some phase if $|k_x\tilde{u}_y - k_y\tilde{u}_x| > 2\Omega$, leading to a local inertial instability. The breaking criterion is again equivalent to $|k_z\tilde{\xi}_z| > 1$. Since $\boldsymbol{\nabla}\cdot\boldsymbol{\xi} = 0$ for internal waves, $|k_z\tilde{\xi}_z|$ is equal to $|\boldsymbol{k}_\mathrm{h}\cdot\tilde{\boldsymbol{\xi}}_\mathrm{h}|$, where 'h' denotes the horizontal components.

Internal wave beams undergo similar breaking instabilities when the amplitude exceeds a critical value (Jouve and Ogilvie 2014; Dauxois et al. 2018). This is particularly relevant when the amplitude is increased by a focusing reflection.

Plane internal waves in an unbounded or periodic domain are in fact unstable at *any* non-zero amplitude in the absence of dissipation (Phillips 1981, and references therein). The *parametric subharmonic instability* involves the destabilization of a pair of secondary plane waves through their coupling with the primary wave. Parametric

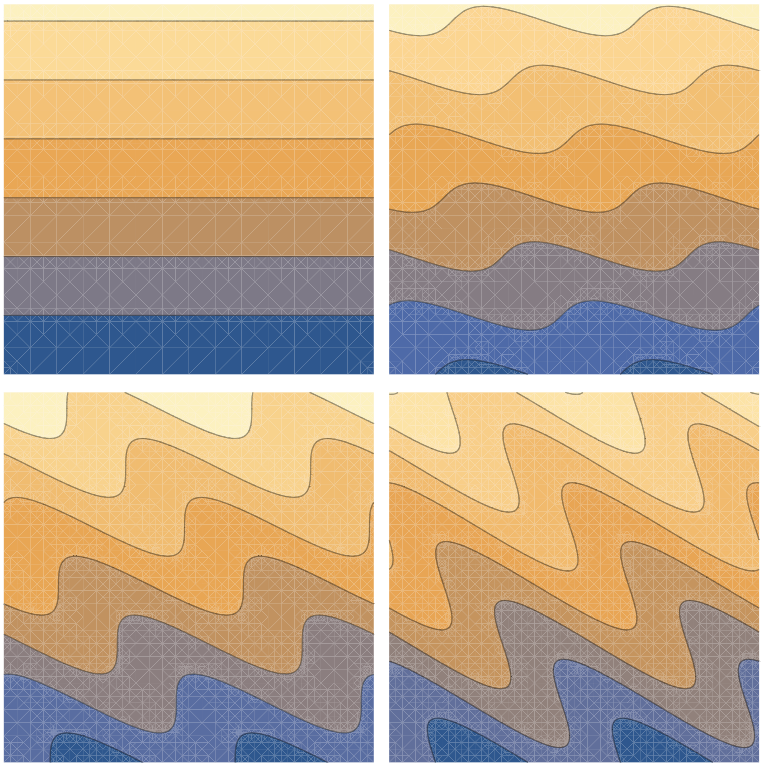

Fig. 1.7 Contours of $z + A\cos(x + z)$ for $A = 0.0$ (top left), 0.5, 1.0 and 1.5 (bottom right). The last case illustrates the overturning of stable stratification by a plane internal wave of sufficient amplitude

resonance occurs if the wavevectors of the three waves sum to zero and similarly for their frequencies, within some tolerance that depends on the amplitude of the primary wave. Owing to the denseness of the spectrum, this condition can always be achieved. However, this type of instability relies on the spatial periodicity of the waves and does not apply to single beams in the same way.

Forced Internal Waves

We have seen that internal waves fill a restricted range of the spectrum of oscillation frequencies in a rotating or stably stratified fluid system, and that the waves may involve singularities. What happens when a system with a dense or continuous spectrum of internal waves is forced at a frequency within that range? For the application to astrophysical tides, we are interested in the total dissipation rate and

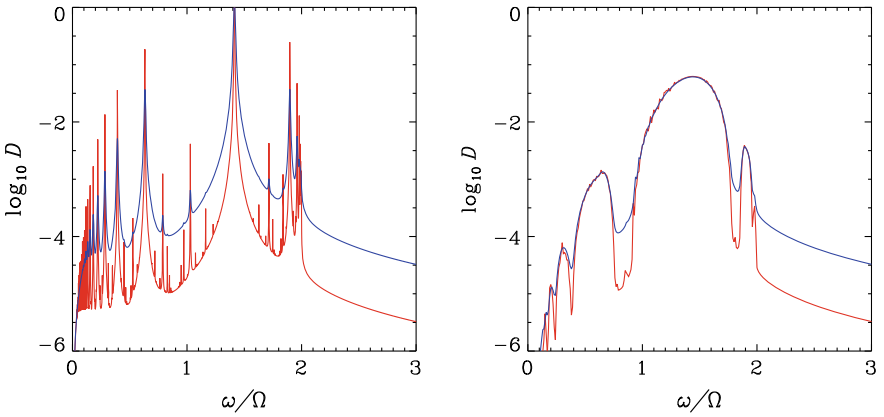

Fig. 1.8 Variation of the dissipation rate (on a logarithmic scale) with forcing frequency, when a rotating fluid in a square domain is subjected to a large-scale body force in the linear regime. The blue and red curves are for frictional damping coefficients $\gamma = 0.01\Omega$ and 0.001Ω, respectively. Left: untilted case, showing classical resonances with separable normal modes in the frequency range of inertial waves. Right: tilted case, showing robust dissipation in wave attractors of finite bandwidth

its dependence on the forcing frequency, especially in the limit that the dissipation coefficients of the fluid are very small.

Figure 1.8 shows the linear response of a rotating fluid in a square container to periodic forcing. The body force is harmonic in time and has a uniform curl. A scale-independent frictional damping is applied to the fluid motion; similar results can be expected for scale-dependent viscous damping. The response curves show the total dissipation rate in a steady state versus the forcing frequency, for two values of the damping coefficient γ.

In the left panel, the rotation axis is aligned with the container and the response is dominated by resonances with normal modes, which have a rectangular structure and can be obtained by separation of variables. Each mode contributes a Lorentzian peak to the dissipation rate, with a height $\propto \gamma^{-1}$ and a width $\propto \gamma$, like a damped harmonic oscillator. In the limit of small γ, the response shows a forest of very narrow peaks, although the frequency-averaged dissipation rate is independent of γ. As expected, the resonances occur at frequencies less than 2Ω.

In the right panel, the rotation axis is tilted by $\arctan(1/3)$ as considered in the section 'Reflections and Singularities'. Now the dissipation rate shows a sequence of smooth, broad ridges. Each is associated with a wave attractor, occupying a certain band of frequency, the broadest of which is the one shown in Fig. 1.5. Within each band, the dissipation rate has a smooth dependence on frequency and becomes independent of γ in the limit $\gamma \to 0$. This behaviour was noted and explained by Ogilvie (2005) using an asymptotic analysis that separates the essentially inviscid large-scale dynamics from the dissipative behaviour on small scales close to the attractor. Large-scale forcing generates waves that are focused towards the attractor and carry a certain energy flux towards it. Provided that there is a mechanism to

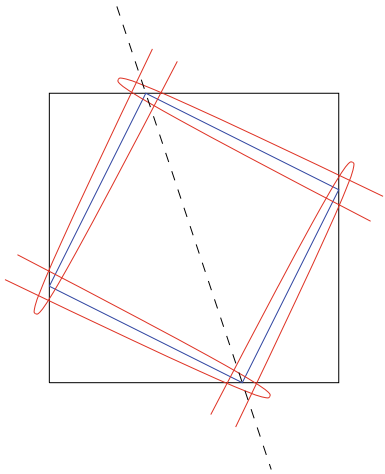

Fig. 1.9 A beam of internal waves (red curves) that achieves a balance between focusing by a wave attractor (blue lines) and viscous spreading

dissipate wave energy on small scales, the attractor absorbs this flux rather like a black hole, without feedback on the large scales. If the dissipation coefficients are lowered, then the waves must undergo more focusing reflections to reach the scale on which they can be dissipated.

Numerical simulations of the tilted square with a viscous fluid (Jouve and Ogilvie 2014) confirm this behaviour in the linear regime. The physics of the forced wave attractor is illustrated in Fig. 1.9. A spreading beam of the type discussed in the section 'Internal Wave Beams', with a virtual source outside the container, is focused at each reflection in a way that compensates exactly for the viscous spreading. The simulations can also explore the nonlinear regime in which the inertial waves become unstable, and it is found that approximately the same total dissipation rate is obtained in the nonlinear regime as if the instability did not occur. As the waves are focused towards the attractor, they reach a length scale on which they become unstable before they can be dissipated directly by viscosity; the instability merely provides an alternative channel of dissipation, by diverting energy into secondary waves of smaller scale that are dissipated more easily by viscosity.

Interiors of Stars and Giant Planets

Interior Models

The interior structure of stars, and their evolution as a result of nuclear reactions, is fairly well understood and described by spherically symmetric, hydrostatic models that neglect rotation and magnetic fields. The structure of the Sun inferred from such models is largely confirmed by helioseismology. It consists of a stably stratified core in which energy is transported by radiation, surrounded by an unstably strat-

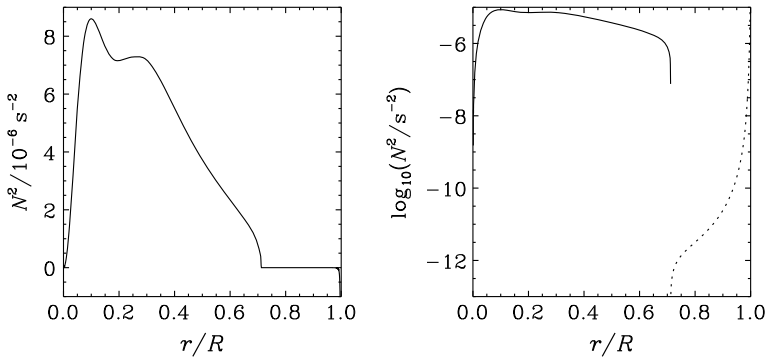

Fig. 1.10 Variation of the squared buoyancy frequency with fractional radius in a standard solar model (Christensen-Dalsgaard et al. 1996). In the logarithmic plot (right), the dashed curve indicates the negative values estimated in the convective zone

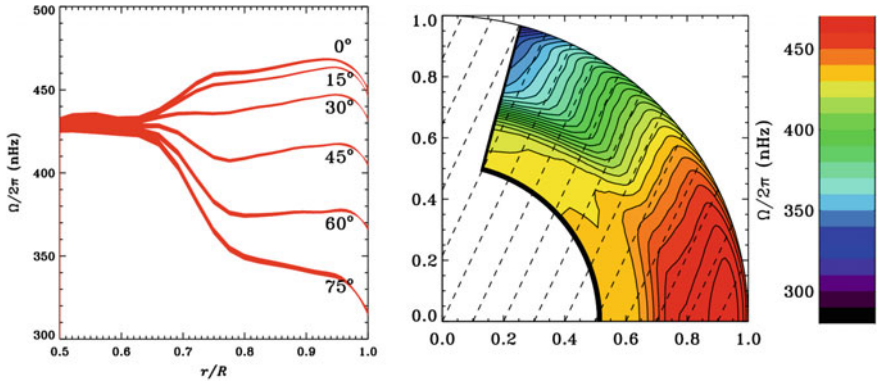

Fig. 1.11 Variation of the solar rotational frequency $\Omega/2\pi$ with radius and latitude, as deduced from helioseismology. Credit: NSO/GONG

ified envelope in which convection dominates. The radial profile of the buoyancy frequency is shown in Fig. 1.10. The distribution of radiative and convective zones varies considerably with the mass and age of the star.

The interior rotation of the Sun has also been deduced from helioseismology, using the rotational splitting of acoustic mode frequencies (Thompson et al. 1996). The latitudinal differential rotation seen at the surface through the motion of sunspots continues nearly to the base of the convective zone (Fig. 1.11).

The interior structure of giant planets, even within the solar system, is much less well understood. Not only are there very few seismological constraints but the interior physics is also more complicated and less certain. Nevertheless, considerable progress has been made recently in modelling the interiors of Jupiter and Saturn (e.g. Helled 2019), and Saturn's rings have been used as a seismometer for the planet (French et al. 2019, and references therein).

Waves and Instabilities in a Stratified, Rotating Body

Basic equations and basic state. The basic equations for an ideal, compressible fluid in cylindrical polar coordinates (r, ϕ, z) are

$$\begin{aligned}
\frac{Du_r}{Dt} - \frac{u_\phi^2}{r} &= -\frac{\partial \Phi}{\partial r} - v\frac{\partial p}{\partial r}, \\
\frac{Du_\phi}{Dt} + \frac{u_r u_\phi}{r} &= -\frac{1}{r}\frac{\partial \Phi}{\partial \phi} - \frac{v}{r}\frac{\partial p}{\partial \phi}, \\
\frac{Du_z}{Dt} &= -\frac{\partial \Phi}{\partial z} - v\frac{\partial p}{\partial z}, \\
\frac{D\ln v}{Dt} = -\frac{1}{\gamma}\frac{D\ln p}{Dt} = \Delta &= \frac{1}{r}\frac{\partial (r u_r)}{\partial r} + \frac{1}{r}\frac{\partial u_\phi}{\partial \phi} + \frac{\partial u_z}{\partial z},
\end{aligned}$$

where

$$\frac{D}{Dt} = \frac{\partial}{\partial t} + u_r\frac{\partial}{\partial r} + \frac{u_\phi}{r}\frac{\partial}{\partial \phi} + u_z\frac{\partial}{\partial z}$$

is the Lagrangian time derivative, $v = 1/\rho$ is the specific volume and γ is the first adiabatic exponent. The gravitational potential Φ is related to the density via Poisson's equation, $\nabla^2\Phi = 4\pi G\rho$.

Consider a steady, axisymmetric basic state representing a (differentially) rotating star or giant plant, described by $v(r, z)$, $p(r, z)$, $\Phi(r, z)$ and $u_\phi = r\Omega(r, z)$, while $u_r = u_z = 0$. This description neglects magnetic fields, convection, meridional circulation, diffusion, etc. Nevertheless, the linear theory of this basic state contains a rich theory of internal waves that is relevant to both free and forced oscillations of stars and giant planets.

The basic equations are satisfied if

$$\begin{aligned}
-r\Omega^2 &= -\frac{\partial \Phi}{\partial r} - v\frac{\partial p}{\partial r}, \\
0 &= -\frac{\partial \Phi}{\partial z} - v\frac{\partial p}{\partial z}.
\end{aligned}$$

The *thermal wind equation* is obtained by eliminating Φ by cross differentiating:

$$-r\frac{\partial \Omega^2}{\partial z} = \frac{\partial v}{\partial r}\frac{\partial p}{\partial z} - \frac{\partial v}{\partial z}\frac{\partial p}{\partial r}.$$

The basic state is called *barotropic* if the right-hand side

$$\frac{\partial(v, p)}{\partial(r, z)} = \boldsymbol{e}_\phi \cdot (\nabla p \times \nabla v)$$

vanishes; otherwise, it is *baroclinic*. According to the fundamental thermodynamic identity $de = T\,ds - p\,dv$ (where e is specific internal energy, T is temperature and s is specific entropy),

$$\frac{\partial(v,\,p)}{\partial(r,\,z)} = \frac{\partial(s,\,T)}{\partial(r,\,z)}, \qquad \nabla p \times \nabla v = \nabla T \times \nabla s.$$

Linearized equations. Now consider small perturbations, representing waves or instabilities on this background. The linearized equations in the *Cowling approximation* (in which perturbations of the gravitational potential are neglected) are

$$\begin{aligned}
\frac{Du_r'}{Dt} - 2\Omega u_\phi' &= -v'\frac{\partial p}{\partial r} - v\frac{\partial p'}{\partial r},\\
\frac{Du_\phi'}{Dt} + u_r'\frac{\partial(r\Omega)}{\partial r} + u_z'\frac{\partial(r\Omega)}{\partial z} + \Omega u_r' &= -\frac{v}{r}\frac{\partial p'}{\partial \phi},\\
\frac{Du_z'}{Dt} &= -v'\frac{\partial p}{\partial z} - v\frac{\partial p'}{\partial z},\\
\frac{Dv'}{Dt} + u_r'\frac{\partial v}{\partial r} + u_z'\frac{\partial v}{\partial z} &= v\Delta',\\
\frac{Dp'}{Dt} + u_r'\frac{\partial p}{\partial r} + u_z'\frac{\partial p}{\partial z} &= -\gamma p\Delta',
\end{aligned}$$

with

$$\frac{D}{Dt} = \frac{\partial}{\partial t} + \Omega\frac{\partial}{\partial \phi}, \qquad \Delta' = \frac{1}{r}\frac{\partial(ru_r')}{\partial r} + \frac{1}{r}\frac{\partial u_\phi'}{\partial \phi} + \frac{\partial u_z'}{\partial z}.$$

Let us introduce the *Lagrangian displacement* $\boldsymbol{\xi}$, which is the difference in position of a fluid element in the perturbed and unperturbed flows. It is related to the Eulerian velocity perturbation $\boldsymbol{u}'$ by

$$\frac{D\boldsymbol{\xi}}{Dt} = \boldsymbol{u}' + \boldsymbol{\xi}\cdot\nabla\boldsymbol{u},$$

or, in components,

$$u_r' = \frac{D\xi_r}{Dt}, \qquad u_\phi' = \frac{D\xi_\phi}{Dt} - r\boldsymbol{\xi}\cdot\nabla\Omega, \qquad u_z' = \frac{D\xi_z}{Dt},$$

and their divergences are related by

$$\Delta' = \nabla\cdot\boldsymbol{u}' = \frac{D}{Dt}(\nabla\cdot\boldsymbol{\xi}).$$

Rewritten in terms of the Lagrangian displacement, the linearized equation of motion has components

$$\frac{D^2\xi_r}{Dt^2} - 2\Omega\frac{D\xi_\phi}{Dt} + 2r\Omega\,\boldsymbol{\xi}\cdot\boldsymbol{\nabla}\Omega = -v'\frac{\partial p}{\partial r} - v\frac{\partial p'}{\partial r},$$
$$\frac{D^2\xi_\phi}{Dt^2} + 2\Omega\frac{D\xi_r}{Dt} = -\frac{v}{r}\frac{\partial p'}{\partial\phi},$$
$$\frac{D^2\xi_z}{Dt^2} = -v'\frac{\partial p}{\partial z} - v\frac{\partial p'}{\partial z},$$

and we find by integration that

$$v' = v\left[\frac{1}{r}\frac{\partial(r\xi_r)}{\partial r} + \frac{1}{r}\frac{\partial\xi_\phi}{\partial\phi} + \frac{\partial\xi_z}{\partial z}\right] - \xi_r\frac{\partial v}{\partial r} - \xi_z\frac{\partial v}{\partial z},$$
$$p' = -\gamma p\left[\frac{1}{r}\frac{\partial(r\xi_r)}{\partial r} + \frac{1}{r}\frac{\partial\xi_\phi}{\partial\phi} + \frac{\partial\xi_z}{\partial z}\right] - \xi_r\frac{\partial p}{\partial r} - \xi_z\frac{\partial p}{\partial z}.$$

Harmonic disturbances. Let us now consider free or forced harmonic disturbances of the form

$$\xi_r = Re\left[\tilde{\xi}_r(r,z)\,\exp(-i\omega t + im\phi)\right],$$

etc., where ω is the wave frequency and m (an integer) is the azimuthal wavenumber. Then, the Lagrangian derivative reduces to multiplication by $-i\hat{\omega}$, where $\hat{\omega} = \omega - m\Omega$ is the *intrinsic wave frequency*: the wave frequency seen in the fluid frame. Dropping the tildes and eliminating ξ_ϕ and v' algebraically, we obtain

$$(-\hat{\omega}^2 + A)\xi_r + B\xi_z = -v\frac{\partial p'}{\partial r} + \frac{vp'}{\gamma p}\frac{\partial p}{\partial r} + \frac{2\Omega}{\hat{\omega}}\frac{v}{r}mp',$$
$$C\xi_r + (-\hat{\omega}^2 + D)\xi_z = -v\frac{\partial p'}{\partial z} + \frac{vp'}{\gamma p}\frac{\partial p}{\partial z},$$
$$\left(1 - \frac{m^2v_s^2}{r^2\hat{\omega}^2}\right)p' = -\gamma p\left[\frac{1}{r}\frac{\partial(r\xi_r)}{\partial r} + \frac{m}{r}\frac{2\Omega}{\hat{\omega}}\xi_r + \frac{\partial\xi_z}{\partial z}\right] - \xi_r\frac{\partial p}{\partial r} - \xi_z\frac{\partial p}{\partial z},$$

where $v_s = \sqrt{\gamma p/\rho}$ is the adiabatic sound speed and the four coefficients are given by

$$A = 4\Omega^2 + r\frac{\partial\Omega^2}{\partial r} - \left(\frac{\partial v}{\partial r} + \frac{v}{\gamma p}\frac{\partial p}{\partial r}\right)\frac{\partial p}{\partial r},$$
$$B = r\frac{\partial\Omega^2}{\partial z} - \left(\frac{\partial v}{\partial z} + \frac{v}{\gamma p}\frac{\partial p}{\partial z}\right)\frac{\partial p}{\partial r},$$
$$C = -\left(\frac{\partial v}{\partial r} + \frac{v}{\gamma p}\frac{\partial p}{\partial r}\right)\frac{\partial p}{\partial z},$$
$$D = -\left(\frac{\partial v}{\partial z} + \frac{v}{\gamma p}\frac{\partial p}{\partial z}\right)\frac{\partial p}{\partial z}.$$

According to the thermal wind equation, $B = C$ and the coefficients form a symmetric matrix

$$\mathbf{M} = \begin{pmatrix} A & B \\ C & D \end{pmatrix} = \begin{pmatrix} A & B \\ B & D \end{pmatrix}.$$

These can be written in terms of gradients of the specific angular momentum $\ell = r^2\Omega$ and the specific entropy s (if the composition is uniform), as well as the effective gravity $\boldsymbol{g} = -\nabla\Phi + r\Omega^2\,\boldsymbol{e}_r = v\nabla p$:

$$\begin{aligned} A &= \frac{1}{r^3}\frac{\partial \ell^2}{\partial r} - \delta\,\frac{g_r}{c_p}\frac{\partial s}{\partial r}, \\ B &= \frac{1}{r^3}\frac{\partial \ell^2}{\partial z} - \delta\,\frac{g_r}{c_p}\frac{\partial s}{\partial z} = -\delta\,\frac{g_z}{c_p}\frac{\partial s}{\partial r}, \\ D &= -\delta\,\frac{g_z}{c_p}\frac{\partial s}{\partial z}, \end{aligned}$$

where we have used

$$\left(\frac{\partial \ln v}{\partial s}\right)_p = \left(\frac{\partial \ln v}{\partial \ln T}\right)_p \left(\frac{\partial \ln T}{\partial s}\right)_p = \delta\,\frac{1}{c_p}$$

and note that $\delta = 1$ for an ideal gas.

Our equations are reducible to a second-order partial differential equation (PDE) for p'. Without writing this out in full, we can note that the structure of the second-derivative terms is

$$(\hat{\omega}^2 - D)\frac{\partial^2 p'}{\partial r^2} + 2B\frac{\partial^2 p'}{\partial r \partial z} + (\hat{\omega}^2 - A)\frac{\partial^2 p'}{\partial z^2} + \cdots = 0,$$

implying that the PDE is hyperbolic when

$$B^2 > (\hat{\omega}^2 - A)(\hat{\omega}^2 - D).$$

This is true for squared frequencies in the range

$$\frac{(A+D) - \sqrt{(A-D)^2 + 4B^2}}{2} < \hat{\omega}^2 < \frac{(A+D) + \sqrt{(A-D)^2 + 4B^2}}{2}, \quad (1.2)$$

corresponding to *inertia-gravity waves*—internal waves that are restored by a combination of inertial and buoyancy forces and generalize the waves discussed in the sections 'Plane Inertial Waves' and 'Plane Internal Gravity Waves'. The characteristics of the hyperbolic PDE are generally curved, unlike those of Poincaré's equation for pure inertial waves in a uniformly rotating fluid.